Available online at http://scik.org
Commun. Math. Biol. Neurosci. 2023, 2023:86
https://doi.org/10.28919/cmbn/7971
ISSN: 2052-2541

GLOBAL STABILITY ANALYSIS AND OPTIMAL PREVENTION OF COVID-19 SPREAD IN GHANA: A COMPARTMENTAL MODELLING PERSPECTIVE

DOMINIC OTOO[1], ALBERT GYAN[1], HAWA ADUSEI[2], DANIEL GYAMFI[1], SHAIBU OSMAN[3,*]

[1]Department of Mathematics and Statistics, University of Energy and Natural Resources, Sunyani, Ghana

[2]Department of Mathematical sciences, Valley View University, Accra, Ghana

[3]Department of Basic Sciences, University of Health and Allied Sciences, Ho, Ghana

Abstract. COVID-19 exposed most of the world healthcare systems as many countries were compelled to request for international support. The disease spreads through contact with bodily fluids of the infected person. COVID-19 poses great threat to people in old age with the disease's severity risks factor borne by them. In this study, we developed a Covid-19 that explains the transmission mechanism of the disease. Model's equilibrium points were determined and local stability analyses of the model at equilibrium was carried out. The analyses showed that disease free-equilibrium is stable when $R_0 < 1$ and unstable when $R_0 > 1$. Global stability analyses were also performed for the models using analytic methods of Lyapunov function approach. The model is then extended to optimal control by adding time-dependent controls. The model was analysed qualitatively with Pontryagin's Maximum principle. Numerical simulations were carried out for the model by designing an iterative scheme that used a fourth-order Runge Kutta method. The numerical analyses also determine the effective strategy in controlling the disease. Best control strategy is education and sensitisation of the public on the dangers and possible causes of the infection.

Keywords: global stability; reproductive rate; equilibrium point; optimal control; Pontryagin's maximum principle; vaccination.

2020 AMS Subject Classification: 34D23.

*Corresponding author

E-mail address: sosman@uhas.edu.gh

Received March 24, 2023

1. INTRODUCTION

The high transmissible viral disease that transcended the nations of the world, and plaguing humanity with respiratory difficulty symptoms and death became a public heath concern in 2020 when WHO confirmed the outbreak in Hubei, China. The disease surge to other nations, with high number of case fatalities recorded in almost every part of the world. COVID-19 exposed most of the world health systems, and caused most countries to request for international support. The disease increased number of bed users as it escalated the condition of those with underlying factors [1].

The disease spreads through contact with bodily fluids of the infected. COVID-19 poses great threat to people in old age, with the disease's severity risks factor borne by them. As a result of the implications of the disease on aged and individuals with underlying factor, the older generation were encouraged to adhere various preventive protocols outlined by the World Health Organization (WHO). In the later parts of 2021, there was a breakthrough in vaccine development, and several vaccines were manufactured to support pharmaceutical intervention of the disease. The vaccine roll outs have drastically lowered the number of COVID cases and reduced hospitalization in many parts of the world. Further, in some cases and regions, the reported compilations induced in the vaccinated host far out weighs the benefits of the vaccines, and that has been hurting the smooth execution of the vaccination programs [2].

Authors in [3] proposed and analysed a compartmental mathematical model on coronavirus infections to predict highest priority for management and control transmission dynamics with limited resources of the COVID-19 or SARS-CoV-2 virus outbreak in India based on accessible data documented within the period of 30th January, 2020 to 30th April, 2020. The basic reproduction number R_0 was computed which further was used to study the model predictions and simulation as the sensitivity indices of the R_0 was conducted to measures the initial transmission of the coronavirus.

Epidemiological models generally explain the transmission dynamics of infections and can predict the persistence or die out of the infection with time. An optimal control can be incorporated into these models to determine the most effective control measures that comes with less costs [4, 5, 6, 7].

Authors in [8] investigated an age-structure mathematical model to quantify effectiveness of social distances interventions within a midsized city in the Europe and United States. However, the study aimed at evaluating effectiveness of these interventions as the study provided estimated proportion of cases, deaths and hospitalizations in medium-sized cities averted within key and short-term challenges as social distancing interventions were in place. The results of the study highlighted timely interventions of social distancing to limits the rate of infection which showed averted in deaths, new cases and hospitalizations with modest reductions contact among the adults population while social intervention strategies were in place.

[9] formulated and proposed a mathematical model that incorporates dynamics behavior of isolation class of the infected humans and risk of future spread of endemic coronavirus infection when it spreads through a community. The model formulated was designed on the assumption that same rate of contacts of the exposed and infection classes with susceptible individuals as the total population was divided into five classes; susceptible class, exposed class, infected class, quarantine individuals and recovered class. The study however discussed the positivity of individual classes with all the solutions of system remained non-negative as $t \geq 0$. The local and global stability of the proposed model were carried out depended on the basic reproduction number.

Authors in [10] studied a mathematical model to investigate the design of optimal control strategies for early severe SARS-CoV-2 transmission based on the data published in Wuhan and surrounding areas. The study first investigated the state-space and epidemic economic concerns and prevention associated with critical parameters were simultaneously considered from different factors. The study also proposed a multi-objective genetic algorithms for efficient optimal design strategies of numerous weights and single cost functions obtained the best solutions were combined.

Researchers in [11] developed a mathematical model using both nonlinear fractional and ordinary differential equation of the novel corona virus disease outbreak in 2019. The study tried to investigate the transmission rate of human to human infection and control measures of the disease. Their model considered simple transmission rate of the infection. Total population is divided into six individuals with natural human mortality into susceptible population. The

results of the nonlinear ordinary differential equation better predict the best-fit and future situation of corona virus in Nigeria.

2. MODEL DESCRIPTION AND FORMULATION

The model is categorized into five compartments based on disease status such as; Susceptible, (S), Exposed, (E_c), Infected, (I_c), Treatment, (T_c) and Recovery, R_c. The model assumes that individuals are recruited into the susceptible population at rate Λ. β is the rate at which susceptible individuals are infected when they come in contact with an infected person. The rate of progression of the disease from the exposed to the infected compartment is given by α. Infected individuals seek treatment at a rate γ, while a fraction of the infected individuals recover and move to the recovery compartment. Treated individual also recover at rate σ. The model assumes that recovered individuals may loss the immunity after some time and becomes susceptible at rate ρ. μ is natural death. Table 1 shows the parameter values used in the Covid-19 model and their descriptions.

TABLE 1. COVID-19 Model and Parameter description

Parameter	**Description**
Λ	The rate at which individuals enter the susceptible population
β	The transmission rate
α	Rate at which exposed people become infected
γ	Recruitment rate into treated compartment
$(1-\gamma)$	Recruitment rate into recovery compartment
σ	Recruitment rate from treated into recovery compartment.
μ	Natural death rate

Based on these assumption, the system of ordinary differential equations for the proposed COVID model in Figure 1 is given by;

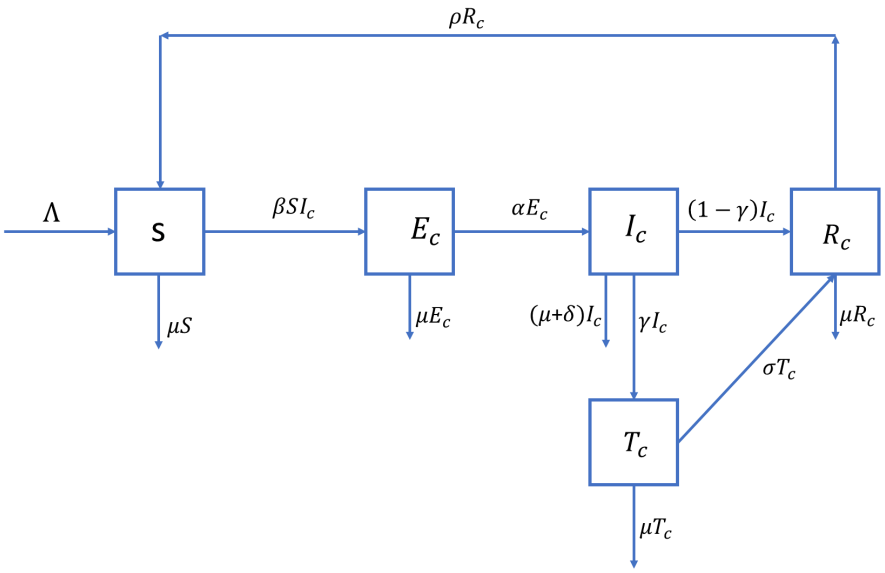

FIGURE 1. Schematic diagram of the COVID Model

$$
(1) \qquad \begin{cases} \frac{d}{dt}S = \Lambda - \beta S I_c - \mu S + \rho R_c \\ \frac{d}{dt}E_c = \beta S I_c - (\mu + \alpha)E_c \\ \frac{d}{dt}I_c = \alpha E_c - (1-\gamma)I_c - (\mu + \delta + \gamma)I_c \\ \frac{d}{dt}T_c = \gamma I_c - (\mu + \sigma)T_c \\ \frac{d}{dt}R_c = \sigma T_c + (1-\gamma)I_c - (\mu + \rho)R_c \end{cases}
$$

3. MODEL ANALYSIS

3.1. Positivity of solutions.

$$
(2) \qquad \frac{ds}{dt} = \quad \Lambda - S(\beta I_c + \mu) + PR_c
$$

$$
\begin{aligned} \frac{ds}{dt} &\geq \quad -S(\beta I_c + \mu) \\ \frac{ds}{s} &\geq \quad -(\beta I_c + \mu)\, d_t \\ \int \frac{ds}{s} &\geq \quad -\int (\beta I_c + \mu)\, d_t \\ ln_s &\geq \quad -(\beta I_c + \mu)t + C \end{aligned}
$$

$$\begin{aligned}
\text{At } t=0, S &= S_0 \\
lnS_0 &= c \\
lnS &\geq -(\beta I_c+\mu)t + lnS_0 \\
lnS - lnS_0 &\geq -(\beta I_c+\mu)t \\
ln\left(\frac{S}{S_0}\right) &\geq -(\beta I_c+\mu)t \\
\frac{S}{S_0} &\geq e^{-(\beta I_c+\mu)t} \\
S &\geq S_0 e^{-(\beta I_c+\mu)t} \\
S &\geq 0
\end{aligned}$$

Same applies for;

$\frac{dE}{dt}, \frac{dI}{dt}, \frac{dR}{dt}, \frac{dT}{dt}$.

Hence;

$E \geq 0, I \geq 0, R \geq 0, T \geq 0$

3.2. Feasibility Region.

$$\begin{aligned}
N &= S+E_c+I_c+T_c+R_c \\
\frac{dN}{dt} &= \frac{ds}{dt}+\frac{dE_c}{dt}+\frac{dI_c}{dt}++\frac{dT_c}{dt}++\frac{dR_c}{dt} \\
\frac{dN}{dt} &= \Lambda-\mu N-\delta I_c-\gamma I_c \\
\frac{dN}{dt} &\leq \Lambda-\mu N \\
\frac{dN}{\Lambda-\mu N} &\leq dt \\
\frac{dN}{-\mu(N-\frac{\Lambda}{\mu})} &\leq dt \\
\frac{dN}{(N-\frac{\Lambda}{\mu})} &\leq -\mu dt \\
ln\left(N-\frac{\Lambda}{\mu}\right) &\leq -\mu t+c \\
At \quad t=0, N &= N_0 \\
ln\left(N_0-\frac{\Lambda}{\mu}\right) &\leq c \\
ln\left(N-\frac{\Lambda}{\mu}\right) &\leq -\mu t+ln\left(N_0-\frac{\Lambda}{\mu}\right) \\
ln\left(\frac{N-\frac{\Lambda}{\mu}}{N_0-\frac{\Lambda}{\mu}}\right) &\leq -\mu t
\end{aligned}$$

$$\begin{aligned}
\left(\frac{N-\frac{\Lambda}{\mu}}{N_0-\frac{\Lambda}{\mu}}\right) &\leq e^{-\mu t} \\
As \quad t \to \infty & \\
\left(\frac{N-\frac{\Lambda}{\mu}}{N_0-\frac{\Lambda}{\mu}}\right) &\leq 0 \\
N-\frac{\Lambda}{\mu} &\leq 0 \\
N &\leq \frac{\Lambda}{\mu}
\end{aligned}$$

Therefore, the positive solution set is an invariant set of the model and is given by;

$$\cap = \left(C_s, E_c, I_c, T_c, R_c \; \varepsilon \; R_+^s : \; N \leq \frac{\Lambda}{\mu}\right) \tag{3}$$

DISEASE-FREE EQUILIBRIUM

When no infection exist in the system 1, then , the system is said to have a disease-free equilibrium. The equilibrium point is given by setting the left hand side of the state system 1 to zero, and solving for each variable of the state system [12, 13]. Hence, we get

$$\begin{cases}
0 = \Lambda - \beta S I_c - \mu S + \rho R_c \\
0 = \beta S I_c - (\mu + \alpha) E_c \\
0 = \alpha E_c - (1-\gamma) I_c - (\mu + \delta + \gamma) I_c \\
0 = \gamma I_c - (\mu + \sigma) T_c \\
0 = \sigma T_c + (1-\gamma) I_c - (\mu + \rho) R_c
\end{cases} \tag{4}$$

Obviously, when there is no infection in the system, $E_c = I_c = T_c = R_c = 0$. Therefore, each compartment of system 4 would be equal to zero except the first compartment. Since $E_c = I_c = T_c = R_c = 0$. Thus, we have

$$\begin{cases} 0 = \Lambda - \mu S \end{cases} \tag{5}$$

From 5, solving for S gives
$S = \dfrac{\Lambda}{\mu}$.
Hence, the disease-free equilibrium point D_0 is given by

$$D_0 = (S_0, E_{c_0}, I_{c_0}, T_{c_0}, R_{c_0}) = (\frac{\Lambda}{\mu}, 0, 0, 0, 0) \tag{6}$$

4. BASIC REPRODUCTION NUMBER R_0

The basic reproductive number is threshold value that governs the persistence or die out of the disease [14, 15, 16, 17]. From model system 1, the infectious compartments are;

$$\begin{aligned}
\frac{d}{dt}E_c &= \beta S I_c - (\mu+\alpha)E_c \\
\frac{d}{dt}I_c &= \alpha E_c - (1-\gamma)I_c - (\mu+\delta+\gamma)I_c \\
\frac{d}{dt}T_c &= \gamma I_c - (\mu+\sigma)T_c
\end{aligned}$$

We refer to the infectious system and derive matrices F and V as follows;

$$\mathscr{F} = \begin{pmatrix} \beta S I_c \\ 0 \\ 0 \end{pmatrix}, \quad \mathscr{V} = \begin{pmatrix} (\mu+\alpha)E_c \\ (\mu+\delta+\gamma)I_c + (1-\gamma)I_c - \gamma E_c \\ (\mu+\sigma)T_c - \gamma I_c \end{pmatrix}$$

The Jacobian matrix of $\mathscr{F}$ is given by

$$\left(\mathscr{F} = \begin{pmatrix} 0 & \beta S & 0 \\ 0 & 0 & 0 \\ 0 & 0 & 0 \end{pmatrix} \right) \tag{7}$$

Evaluating Matrix $\mathscr{F}$ at the disease free equilibrium $(S_0, E_{c_0}, I_{c_0}, T_{c_0}, R_{c_0}) = (\frac{\Lambda}{\mu}, 0, 0, 0, 0)$ gives

$$F = \begin{pmatrix} 0 & \beta\frac{\Lambda}{\mu} & 0 \\ 0 & 0 & 0 \\ 0 & 0 & 0 \end{pmatrix}$$

In the same way, the Jacobian of the matrix $\mathscr{V}$ is given by

$$\mathscr{V} = \begin{pmatrix} (\mu+\alpha) & 0 & 0 \\ -\alpha & (\mu+\delta+\gamma)+(1-\gamma) & 0 \\ 0 & 0 & (\mu+\sigma)-\gamma \end{pmatrix} \tag{8}$$

Evaluating matrix $\mathscr{V}$ at the disease free equilibrium $(S_0, E_{c_0}, I_{c_0}, T_{c_0}, R_{c_0}) = (\frac{\Lambda}{\mu}, 0, 0, 0, 0)$ gives

$$\mathscr{V} = \begin{pmatrix} (\mu+\alpha) & 0 & 0 \\ -\alpha & (\mu+\delta+\gamma)+(1-\gamma) & 0 \\ 0 & 0 & (\mu+\sigma)-\gamma \end{pmatrix} \tag{9}$$

The inverse matrix of the matrix $\mathscr{V}$ is given by

$$V^{-\prime} = \begin{pmatrix} \frac{1}{(\mu+\alpha)} & 0 & 0 \\ \frac{\alpha}{(\mu+\alpha)(\mu+\delta+\gamma)+(1-\gamma)} & \frac{1}{(\mu+\delta+\gamma)+(1-\gamma)} & 0 \\ 0 & 0 & \frac{1}{(\mu+\sigma)-\gamma} \end{pmatrix} \tag{10}$$

Now,

(11)

$$FV^{-\prime} = \begin{pmatrix} 0 & \beta\frac{\Lambda}{\mu} & 0 \\ 0 & 0 & 0 \\ 0 & 0 & 0 \end{pmatrix} \begin{pmatrix} \frac{1}{(\mu+\alpha)} & 0 & 0 \\ \frac{\alpha}{(\mu+\alpha)(\mu+\delta+\gamma)+(1-\gamma)} & \frac{1}{(\mu+\delta+\gamma)+(1-\gamma)} & 0 \\ 0 & 0 & \frac{1}{(\mu+\sigma)-\gamma} \end{pmatrix}$$

Hence, the basic reproduction number R_0 is given by

$$R_0 = \frac{\beta\Lambda}{\mu(\mu+\alpha)\big((\mu+\delta+\gamma)+(1-\gamma)\big)}$$

4.1. Endemic equilibrium. When the disease under consideration exists in the system, the system is likely to be endemic at the long run. Endemic equilibrium $E_Q = (S^*, E_C^*, I_C^*, T_C^*, R_C^*)$ of the COVID model system 1 given is

$$S^* = \frac{\Lambda+\rho R_c^*}{\beta I_c^*+\mu},$$

$$E_c^* = \frac{\beta S^* I_c^*}{\mu+\alpha},$$

$$I_c^* = \frac{\alpha E_c^*}{(\mu+\alpha)(\mu+\delta+\gamma)+(1-\gamma)},$$

$$T_c^* = \frac{\gamma I_c^*}{(\mu+\alpha)},$$

$$R_c^* = \frac{\sigma T_c^*+(1-\gamma)I_c^*}{\mu+\rho}.$$

4.2. Stability analysis at the disease free equilibrium. The subsection 4.2 examines the stability of the the model system (1) at the disease-free equilibrium. The linearization method is employed to study the model system (1) stability. Using the linearised Jacobian matrix L_{J_D} is given by

$$L_{J_D} = \begin{pmatrix} -\beta I_c - \mu & 0 & -\beta S & 0 & \rho \\ \beta I_c & -(\mu+\alpha) & \beta S & 0 & 0 \\ 0 & \alpha & -(1-\gamma)-(\mu+\delta+\gamma) & 0 & 0 \\ 0 & 0 & \gamma & -(\mu+\sigma) & 0 \\ 0 & 0 & (1-\gamma) & \sigma & (-\mu+\rho) \end{pmatrix} \tag{12}$$

When the Jacobian 12 is evaluated at the disease-free equilibrium $(\frac{\Lambda}{\mu},0,0,0,0)$, the following matrix is generated;

$$(A-\lambda I) = \begin{pmatrix} -\mu-\lambda & 0 & -\beta\frac{\Lambda}{\mu} & 0 & \rho \\ 0 & -(\mu+\alpha)-\lambda & \beta\frac{\Lambda}{\mu} & 0 & 0 \\ 0 & \alpha & -(1-\gamma)-(\mu+\delta+\gamma)-\lambda & 0 & 0 \\ 0 & 0 & \gamma & -(\mu+\sigma)-\lambda & 0 \\ 0 & 0 & (1-\gamma) & \sigma & -(\mu+\rho)-\lambda \end{pmatrix} \tag{13}$$

Clearly, $\lambda_1 = -\mu$,$\lambda_2 = -(\mu+\rho)$,$\lambda_3 = -(\mu+\sigma)$,

It follows that the remaining matrix is given by

$$\mathscr{H} = \begin{pmatrix} -(\mu+\alpha)-\lambda & \beta\frac{\Lambda}{\mu} \\ \alpha & -(1-\gamma)-(\mu+\delta+\gamma)-\lambda \end{pmatrix} \tag{14}$$

Matrix 14 is strictly diagonally dominant since $|-(\mu+\alpha)-\lambda| > \beta\frac{\Lambda}{\mu}$ and $|-(1-\gamma)-(\mu+\delta+\gamma)-\lambda| > \alpha$. Hence, from Gershgorin circle theorem **??**, model system 1 is locally asymptotically stable at the disease free equilibrium.

5. Global Stability of the Disease-Free Equilibrium

The subsection 5 studies the stability of the disease-free equilibrium of model system 1 by constructing a suitable Lyapunov function for the model 1.

Theorem 1. *The disease-free equilibrium* $D_0 = (S_0, E_{c_0}, I_{c_0}, T_{c_0}, R_{c_0}) = (\frac{\Lambda}{\mu}, 0, 0, 0, 0)$ *is globally asymptotically stable in* R^5_+ *if* $R_0 < 1$.

Proof. We construct a Lyapunov function $L(S, E_C, I_C, T_C, R_C) : R^5 \to R^+$, for disease-free equilibrium point defined as

$$L = \big(\frac{1}{d_1 d_2}\big) E_C + \frac{1}{d_2}\big(\frac{I_C}{\alpha}\big), \tag{15}$$

where $d_1 = (\mu + \alpha)$, $d_2 = \big((\mu + \delta + \gamma) + (1 - \gamma)\big)$

$$\frac{dL}{dt} = \big(\frac{1}{d_1 d_2}\big)\frac{dE_C}{dt} + \frac{1}{d_2 \alpha}\frac{dI_C}{dt}, \tag{16}$$

$$\frac{dL}{dt} = \big(\frac{1}{d_1 d_2}\big)(\beta S I_c - (\mu + \alpha)E_c) + \frac{1}{d_2 \alpha}(\alpha E_c - (1 - \gamma)I_c - (\mu + \delta + \gamma)I_c), \tag{17}$$

$$\frac{dL}{dt} = \big(\frac{1}{d_1 d_2}\big)(\beta S I_c - d_1 E_c) + \frac{1}{d_2 \alpha}(\alpha E_c - d_2 I_c),$$

$$\frac{dL}{dt} = \big(\frac{1}{d_1 d_2}\big)(\beta S I_c) - \big(\frac{1}{d_2}\big)(E_c) + \frac{1}{d_2 \alpha}(\alpha E_c) - \frac{1}{\alpha}(I_c),$$

$$\frac{dL}{dt} = \big(\frac{1}{d_1 d_2}\big)(\beta S I_c) - \frac{1}{\alpha}(I_c), \tag{18}$$

But $s = \dfrac{\Lambda}{\mu}$ at the disease-free equilibrium. Hence,

$$\frac{dL}{dt} = \big(\frac{1}{d_1 d_2}\big)\beta\frac{\Lambda}{\mu} I_c - \frac{1}{\alpha}(I_c), \tag{19}$$

$$\frac{dL}{dt} = R_0 I_c - \frac{1}{\alpha}(I_c),$$

$$\frac{dL}{dt} = (R_0 - \frac{1}{\alpha})I_c, \tag{20}$$

It follows that $\dfrac{dL}{dt} \leq 0$ when $\alpha < 1$ for $R_0 < 1$. Further, it can be noted that $\dfrac{dL}{dt} = 0$, when $I_c = 0$. Hence, from [**?**], the disease-free equilibrium, D_0 is globally asymptotically stable when $R_0 < 1$. □

6. STABILITY-ENDEMIC EQUILIBRIUM

The subsection 6 studies the stability of the COVID model system 1 at the endemic equilibrium. Model system 1 would be linearised by Linearisation approach [18, 19, 20]. The Jacobian matrix is given by

$$\begin{pmatrix} -\beta I_c^* - \mu & 0 & -\beta S^* & 0 & \rho \\ \beta I_c^* & -(\mu+\alpha) & \beta S^* & 0 & 0 \\ 0 & \alpha & -(1-\gamma)-(\mu+\delta+\gamma) & 0 & 0 \\ 0 & 0 & \gamma & -(\mu+\sigma) & 0 \\ 0 & 0 & (1-\gamma) & \sigma & (-\mu+\rho) \end{pmatrix} \tag{21}$$

Hence, $(A-qI)$ becomes

$$\begin{pmatrix} -(\beta I_c^* - \mu) - q & 0 & -\beta S^* & 0 & \rho \\ \beta I_c^* & -(\mu+\alpha) - q & \beta S^* & 0 & 0 \\ 0 & \alpha & -\big((1-\gamma)-(\mu+\delta+\gamma)\big) - q & 0 & 0 \\ 0 & 0 & \gamma & -(\mu+\sigma) - q & 0 \\ 0 & 0 & (1-\gamma) & \sigma & (-\mu+\rho) - q \end{pmatrix} \tag{22}$$

The real part of matrix 22 eigenvalues would not be negative since the matrix 22 is not strictly diagonally dominant. Hence, by Gershgorin circle theorem [21], model system 1 is unstable.

6.1. Global Stability of the endemic equilibrium.

The subsection 6.1 examines the global stability of the endemic equilibruim of the COVID model (1) by constructing a suitable Lyapunov function for model system model (1). The analysis is given as follows.

Theorem 2. *Given that $S = S^*$, $E_C = E_C^*$, $I_C = I_C^*$, $T_C = T_C^*$, and $R_C = R_C^*$, then, the endemic equilibrium E_Q^* of the COVID model (1)is globally asymptotically stable in $R+^5$ whenever $R_0 > 1$.*

Proof. We define a lyapunov function

$$L : \{(S, E_C, I_C, T_C, R_C) \in \varphi \| S, E_C, I_C, T_C, R_C > 0\} \to R \tag{23}$$

given by

$$L(S,E_C,I_C,T_C,R_C) = \big(S-S^*-S^*ln\frac{S}{S^*}\big)+\big(E_C-E_C^*-E_C^*ln\frac{E_C}{E_C^*}\big)+\big(I_C-I_C^*-I_C^*ln\frac{I_C}{I_C^*}\big)$$
$$+\big(T_C-T_C^*-T_C^*ln\frac{T_C}{T_C^*}\big)+\big(R_C-R_C^*-R_C^*ln\frac{R_C}{R_C^*}\big)$$

The time derivative of L becomes

(24)
$$\frac{dL}{dt} = \big(\frac{S-S^*}{S}\big)\frac{dS}{dt}+\big(\frac{E_C-E_C^*}{E_C}\big)\frac{dE_C}{dt}+\big(\frac{I_C-I_C^*}{I_C}\big)\frac{dI_C}{dt}+\big(\frac{T_C-T_C^*}{T_C}\big)\frac{dT_c}{dt}+\big(\frac{R_C-R_C^*}{R_C}\big)\frac{dR_C}{dt}$$

$$\begin{aligned}\frac{dL}{dt} &= \big(\frac{S-S^*}{S}\big)\big(\Lambda-\beta(S-S^*)(I_c-I_c^*)-\mu(S-S^*)+\rho(R_c-R_c^*)\big)\\ &+\big(\frac{E_C-E_C^*}{E_C}\big)\big(\beta(S-S^*)(I_c-I_c^*)-(\mu+\alpha)(E_c-E_c^*)\big)\\ &+\big(\frac{I_C-I_C^*}{I_C}\big)\big(\alpha(E_c-E_c^*)-(1-\gamma)(I_c-I_c^*)-(\mu+\delta+\gamma)(I_c-I_c^*)\big)\\ &+\big(\frac{T_C-T_C^*}{T_C}\big)\big(\gamma(I_c-I_c^*)-(\mu+\sigma)(T_c-T_c^*)\big)\\ &+\big(\frac{R_C-R_C^*}{R_C}\big)\big(\sigma(T_c-T_c^*)+(1-\gamma)(I_c-I_c^*)-(\mu+\rho)(R_c-R_c^*)\big)\end{aligned}$$

$$\begin{aligned}\frac{dL}{dt} &= \big(\Lambda\big(\frac{S-S^*}{S}\big)-\beta\big(\frac{(S-S^*)^2}{S}\big)(I_c-I_c^*)-\mu\big(\frac{(S-S^*)^2}{S}\big)+\rho(R_c-R_c^*)\big(\frac{S-S^*}{S}\big)\big)\\ &+\big(\beta(S-S^*)\big(\frac{E_C-E_C^*}{E_C}\big)(I_c-I_c^*)-(\mu+\alpha)\big(\frac{(E_C-E_C^*)^2}{E_C}\big)\big)\\ &+\big(\alpha(E_c-E_c^*)\big(\frac{I_C-I_C^*}{I_C}\big)-(1-\gamma)\big(\frac{(I_C-I_C^*)^2}{I_C}\big)-(\mu+\delta+\gamma)\big(\frac{(I_C-I_C^*)^2}{I_C}\big)\big)\\ &+\big(\gamma(I_c-I_c^*)\big(\frac{T_C-T_C^*}{T_C}\big)-(\mu+\sigma)\big(\frac{(T_C-T_C^*)^2}{T_C}\big)\\ &+\big(\sigma(T_c-T_c^*)\big(\frac{R_C-R_C^*}{R_C}\big)+(1-\gamma)(I_c-I_c^*)\big(\frac{R_C-R_C^*}{R_C}\big)-(\mu+\rho)\big(\frac{(R_C-R_C^*)^2}{R_C}\big)\big)\end{aligned}$$

$$\begin{aligned}\frac{dL}{dt} &= \big(\Lambda-\Lambda\big(\frac{S^*}{S}\big)-\beta\big(\frac{(S-S^*)^2}{S}\big)(I_c-I_c^*)-\mu\big(\frac{(S-S^*)^2}{S}\big)+\rho(R_c-R_c^*)\big(\frac{S-S^*}{S}\big)\big)\\ &+\big(\beta(S-S^*)\big(\frac{E_C-E_C^*}{E_C}\big)(I_c-I_c^*)-(\mu+\alpha)\big(\frac{(E_C-E_C^*)^2}{E_C}\big)\big)\\ &+\big(\alpha(E_c-E_c^*)\big(\frac{I_C-I_C^*}{I_C}\big)-(1-\gamma)\big(\frac{(I_C-I_C^*)^2}{I_C}\big)-(\mu+\delta+\gamma)\big(\frac{(I_C-I_C^*)^2}{I_C}\big)\big)\end{aligned}$$

$$+\big(\gamma(I_c-I_c^*)\big(\frac{T_C-T_C^*}{T_C}\big)-(\mu+\sigma)\big(\frac{(T_C-T_C^*)^2}{T_C}\big)$$
$$+\big(\sigma(T_c-T_c^*)\big(\frac{R_C-R_C^*}{R_C}\big)+(1-\gamma)(I_c-I_c^*)\big(\frac{R_C-R_C^*}{R_C}\big)-(\mu+\rho)\big(\frac{(R_C-R_C^*)^2}{R_C}\big)\big)$$

Using the relation $d=d_1-d_2$ give

$$d_1=\Lambda+\rho(R_c-R_c^*)\big(\frac{S-S^*}{S}\big)+\big(\beta(S-S^*)\big(\frac{E_C-E_C^*}{E_C}\big)(I_c-I_c^*)+\big(\alpha(E_c-E_c^*)\big(\frac{I_C-I_C^*}{I_C}\big)$$
$$+\big(\gamma(I_c-I_c^*)\big(\frac{T_C-T_C^*}{T_C}\big)+\big(\sigma(T_c-T_c^*)\big(\frac{R_C-R_C^*}{R_C}\big)+(1-\gamma)(I_c-I_c^*)\big(\frac{R_C-R_C^*}{R_C}\big)$$

and

(25)
$$\begin{aligned} d_2 &= \Lambda\big(\frac{S^*}{S}\big)+\beta\big(\frac{(S-S^*)^2}{S}\big)(I_c-I_c^*)+\mu\big(\frac{(S-S^*)^2}{S}\big)+(\mu+\alpha)\big(\frac{(E_C-E_C^*)^2}{E_C}\big)+(1-\gamma)\big(\frac{(I_C-I_C^*)^2}{I_C}\big) \\ &+ (\mu+\delta+\gamma)\big(\frac{(I_C-I_C^*)^2}{I_C}\big)+(\mu+\sigma)\big(\frac{(T_C-T_C^*)^2}{T_C}\big)+(\mu+\rho)\big(\frac{(R_C-R_C^*)^2}{R_C}\big) \end{aligned}$$

As observed the $d_1<d_2$, which implies that $\frac{dL}{dt}\leq 0$ if $d_1<d_2$. Hence, it follows that $\frac{dL}{dt}=0$ when $S=S^*$, $E_C=E_C^*$, $I_C=I_C^*$, $T_C=T_C^*$, and $R_C=R_C^*$. Therefore the largest compact invariant set $\{S,E_C,I_C,T_C,R_C\in\Delta:\frac{dL}{dt}=0\}$ is the singleton E_Q, where E_Q is the endemic equilibrium. Hence from [22], EQ is globally asymptotically stable in Δ. □

6.2. Sensitivity Analysis. A normalised forward sensitivity index of a variable y, which solely depends deferentially on a parameter x, defined as;

(26)
$$\mathscr{A}_x^y=\frac{\partial y}{\partial x}*\frac{x}{y}$$

TABLE 2. **Covid-19 model parameters and sensitivity index**

Parameters	**Sensitivity index (+ve/-ve)**
Λ	+
β	+
α	+
γ	-
σ	+
δ	+

The most sensitive parameter is the recruitment rate of individuals into the susceptible compartment as in the analysis of Table 2.

7. COVID-19 MODEL EXTENSION TO OPTIMAL CONTROL

The subsection 7 construct an optimal control model for the state model 1 by introducing a time-dependent controls of u_1, denoting education and u_2, denotes a vaccination control. Control model assesses the performance of the considered controls in minimizing the exposed, infected and treated individuals. Hence, the following nonlinear differential equation model is derived;

$$\begin{cases} \frac{d}{dt}S = \Lambda - (1-u_1)\beta SI_c - \mu S + \rho R_c - u_2 S \\ \frac{d}{dt}E_c = (1-u_1)\beta SI_c - (\mu+\alpha)E_c \\ \frac{d}{dt}I_c = \alpha E_c - (1-\gamma)I_c - (\mu+\delta+\gamma)I_c \\ \frac{d}{dt}T_c = \gamma I_c - (\mu+\sigma)T_c \\ \frac{d}{dt}R_c = \sigma T_c + (1-\gamma)I_c - (\mu+\rho)R_c + u_2 S \end{cases} \tag{27}$$

With the main objective of minimizing the exposed, infected and treated individuals, we consider a quadratic function as in [23, 4], that minimizes the exposed, infected and treated individuals through education u_1 and vaccination u_2. Hence, the objective functional $\mathscr{J}$ is given by;

$$J(u_1,u_2) = \int_o^{tf} \left[H_1E_c + H_2I_c + H_3T_c + \frac{1}{2}(D_1u_1^2 + D_2u_2^2) \right].dt \tag{28}$$

Considering the objective functional (28), the quantities H_1, H_2 and H_3 are the weight constants of the exposed, infected and treated individuals. In addition, the terms $\frac{D_1u_1^2}{2}$, and $\frac{D_2u_2^2}{2}$ are the cost that comes with minimizing the exposed, infected and treated individuals. Hence, we seek an optimal control u_1^*, u_2^* such that

$$J(u_1^*,u_2^*) = min\{J(u_1,u_2) : (u_1,u_2) \in U\} \tag{29}$$

where

$$U = \{(u_1,u_2) |\ 0 \leq u_i \leq 1, i = 1,2, \text{ Lebesgue measurable}\} \tag{30}$$

Now, the analytic method of Pontryagin's maximum principle [24], would be employed to converts system 27 and 28 into a problem of minimizing the Hamiltonian H with respect to the controls u_1 and u_2, where;

$$\begin{aligned} H_f = & \left[H_1E_c + H_2I_c + H_3T_c + \frac{1}{2}(D_1u_1^2 + D_2u_2^2)\right] \\ & + \lambda_1\{\Lambda - (1-u_1)\beta SI_c - \mu S + \rho R_c - u_2S\} \\ & + \lambda_2\{(1-u_1)\beta SI_c - (\mu+\alpha)E_c\} \\ & + \lambda_3\{\alpha E_c - (1-\gamma)I_c - (\mu+\delta+\gamma)I_c\} \\ & + \lambda_4\{\gamma I_c - (\mu+\sigma)T_c\} \\ & + \lambda_5\{\sigma T_c + (1-\gamma)I_c - (\mu+\rho)R_c + u_2S\}, \end{aligned} \tag{31}$$

Theorem 3. *There exists an optimal control $U^* = (u_1^*, u_2^*) \in U$ such that*

$$\mathscr{J}(u_1^*, u_2^*) = \min_U \mathscr{J}(u_1, u_2), \tag{32}$$

subject to the control system (27) with the initial conditions.

Proof. We refer to the work by [25] to prove the existence of optimal control of model 37. As observed, the state and control variables are non-negative. We also observe that in minimizing the control problem, the necessary and convexity of the objective functional in u_1 and u_2 are satisfied. The control space

$U = \{u | u_1, u_2$ are measurable, $0 \leq u_1, u_2 \leq u_max < \infty,\ t \in [0, t_f]\}$

is also convex and closed by definition. The optimal system is bounded which verifies the compactness needed for existence of the optimal control. Also, the integrand in the functional 28, $\left[H_1E_c + H_2I_c + H_3T_c + \frac{1}{2}(D_1u_1^2 + D_2u_2^2)\right]$ is convex on the control u. Therefore, we see that there exist a constant $q > 1$, positive numbers u_1 and u_2 such that,

$J(u_1, u_2) \geq u_1\left(|u_1|^2 + |u_2|^2\right)\frac{q}{2} - u^2$.

Hence, there exist an optimal control. In the quest to find optimal solution, the Pontryagin's maximum principle [24] is applied to the Hamiltonian 31 such that if (x, u) is an optimal solution of the optimal control problem, then there exist a non-trivial vector function $\lambda = (\lambda_1 \ \ldots \ \lambda_5)$

satisfying the below equation;

$$\begin{aligned} \frac{dz}{dt} &= \frac{\partial H(t,x,u,\lambda)}{\partial \lambda} \\ 0 &= \frac{\partial H(t,x,u,\lambda)}{\partial u} \\ \frac{d\lambda}{dt} &= -\frac{\partial H(t,x,u,\lambda)}{\partial z} \end{aligned} \tag{33}$$

Hence, the necessary condition associated to the Hamiltonian (31) is applied.

Theorem 4. *Given that S, E_c, I_c, T_c and R_C are optimal state solutions with associated optimal control variables (u_1^*, u_2^*) for the optimal control problem 27 and 28, then there exist adjoint variables λ_i for $i = 1, \ldots, 5$, satisfying;*

$$\begin{aligned} \lambda_1' &= -\frac{\partial H}{\partial S} = (\lambda_1 - \lambda_2)(1-u_1)\beta I_C + (\lambda_1 - \lambda_5)u_2 + \mu\lambda_1 \\ \lambda_2' &= -\frac{\partial H}{\partial E_c} = (\lambda_2 - \lambda_3)\alpha + \mu\lambda_2 - H_1 \\ \lambda_3' &= -\frac{\partial H}{\partial I_c} = (\lambda_1 - \lambda_2)(1-u_1)\beta S + (\lambda_3 - \lambda_5)(1-\alpha) + (\lambda_3 - \lambda_4)\gamma + (\mu+\delta)\lambda_3 - H_2 \\ \lambda_4' &= -\frac{\partial H}{\partial T_c} = (\lambda_4 - \lambda_5)\sigma + \mu\lambda_4 - H_3 \\ \lambda_5' &= -\frac{\partial H}{\partial R_c} = (\lambda_5 - \lambda_1)\rho + \mu\lambda_5 \end{aligned} \tag{34}$$

with boundary condition;

$$\lambda_i(t_f) = 0, \ \mathrm{i} = 1, 2, \ldots, 5 \tag{35}$$

The optimal control u_1^* and u_2^* are given by

$$\begin{aligned} u_1' &= min\left\{1, max\left\{0, \left((\lambda_2 - \lambda_1)\frac{\beta S I_C}{D_1}\right)\right\}\right\} \\ u_2' &= min\left\{1, max\left\{0, \left((\lambda_1 - \lambda_5)\frac{S}{D_2}\right)\right\}\right\} \end{aligned} \tag{36}$$

□

Proof. The adjoint and boundary conditions are derived by applying the Hamiltonian 31. Thus we equate $S = S^*$, $E_c = E_c^*$, $I_c = I_c^*$, $T_C = T_c^*$, and $R_C = R_C^*$ and differentiating the Hamiltonain

with respect to S, E_c, I_c, T_c and R_C to obtain 34. Further, the equations $\frac{\partial H}{\partial u_1} = 0$ and $\frac{\partial H}{\partial u_2} = 0$ are determined on the interior of the control set and using the optimal conditions and the property of the control space u_1 and u_2, and we derive 36. From 36, The control is characterize by solving the optimal system. Thus, the transversality and the characterization of the optimal control (u_1, u_2) are use in solving the optimal system. □

The controls u_1^* and u_2^* when substituted into the control system (37) gives;

$$
(37) \quad \begin{cases} \frac{d}{dt}S &= \Lambda - \left(1 - min\left\{1, max\left\{0, \left((\lambda_2 - \lambda_1)\frac{\beta S I_C}{D_1}\right)\right\}\right\}\right)\beta S I_c - \mu S \\ &\quad + \rho R_c - min\left\{1, max\left\{0, \left((\lambda_1 - \lambda_5)\frac{S}{D_2}\right)\right\}\right\}S \\ \frac{d}{dt}E_c &= \left(1 - min\left\{1, max\left\{0, \left((\lambda_2 - \lambda_1)\frac{\beta S I_C}{D_1}\right)\right\}\right\}\right)\beta S I_c - (\mu + \alpha)E_c \\ \frac{d}{dt}I_c &= \alpha E_c - (1-\gamma)I_c - (\mu + \delta + \gamma)I_c \\ \frac{d}{dt}T_c &= \gamma I_c - (\mu + \sigma)T_c \\ \frac{d}{dt}R_c &= \sigma T_c + (1-\gamma)I_c - (\mu + \rho)R_c + min\left\{1, max\left\{0, \left((\lambda_1 - \lambda_5)\frac{S}{D_2}\right)\right\}\right\}S \end{cases}
$$

8. Numerical Results

We conduct numerical simulations on optimal control strategies on the Cov-19 model using parameter values in 3. This is done by solving the optimal system consisting of state equations 27, the objective functional 28, adjoint equations 33, transversality conditions 34 and the characterisation 36. This is done by applying an iterative scheme using a fourth order Range-Kutta to solve state equations by guessing controls over time [21].

TABLE 3. COVID-19 Model and Parameters

Parameter	Baseline	Source
Λ	$(10-1000)$	[26].
β	1.8980	estimated
α	1.8228	estimated
γ	0.074	[27]
σ	0.0083	[27]
δ	0.15	[26]
μ	0.000042578	[26]

8.1. Effects of varying contact rate β on populations. Generally, contact rate, β has an effect on disease transmission. We look at this effects on the dynamics of disease transmission by varying the contact rate. Figure 2 shows the effects of β on susceptible and infected Covid-19 populations with time.

A decrease in the value of β corresponds to a decrease in susceptible Covid-19 population. However, an increase in the value of β corresponds to an increase in susceptible population. As the value of β increases, there is a corresponding increment in Covid-19 infected population as indicated in Figure 2.

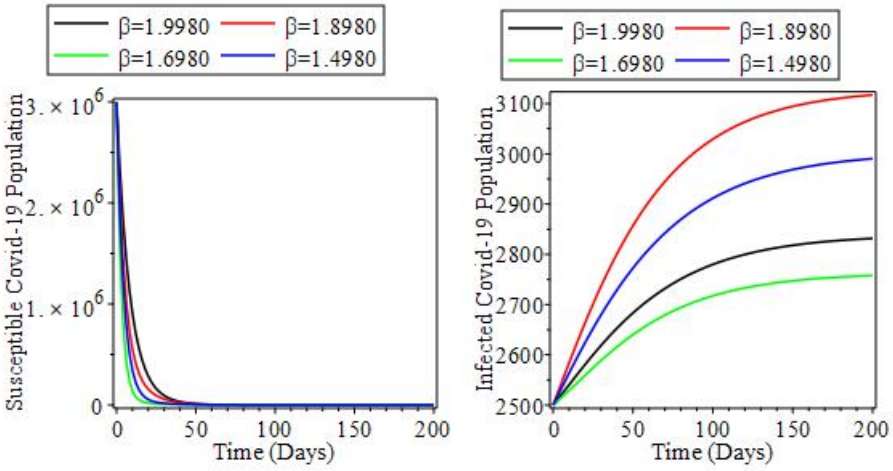

FIGURE 2. Effects of varying contact rate

.

8.2. Strategy 1: Optimal vaccination of susceptible population. Using vaccination control on susceptible population, we optimise the objective functional by setting the other control to zero. This has an effects on susceptible, exposed, treated, and Covid-19 infected populations as shown in Figure 3 and 4 respectively.

There have been an increase in susceptible population as a result of vaccination and a decrease in the number of population infected with the disease. Moreover, populations exposed to the infection have reduced exponentially as indicated in Figure 4.

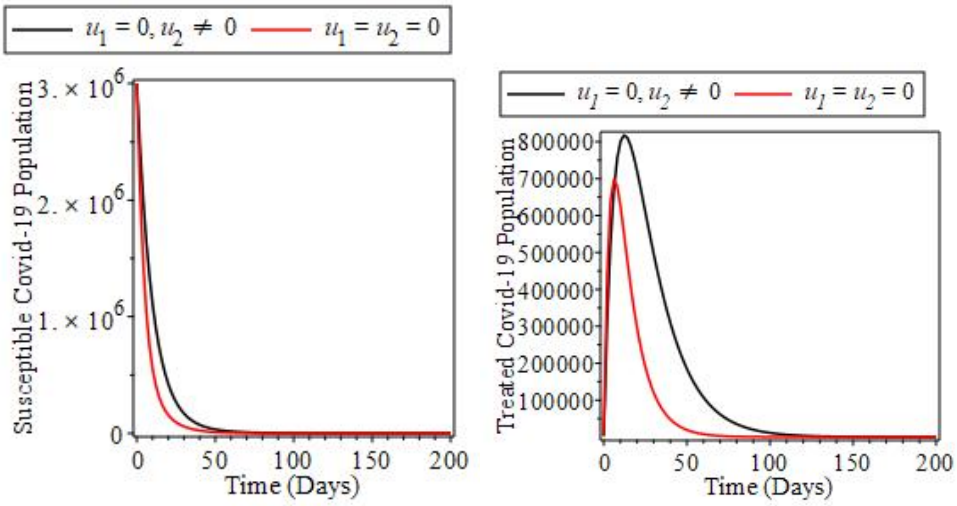

FIGURE 3. plot of phase portraits with u_1 and u_2

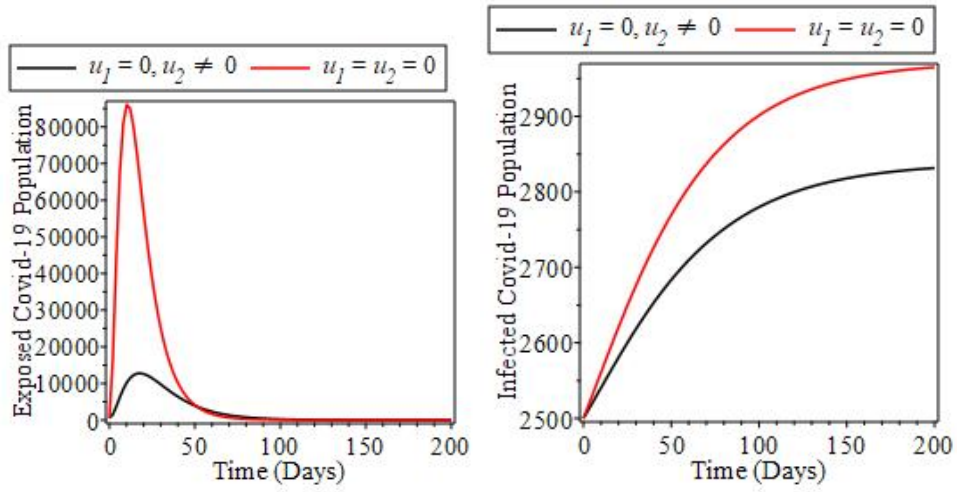

FIGURE 4. plot of phase portraits with u_1 and u_2

8.3. Strategy 2: Optimal education/sensitisation of susceptible population. Using education as a control on susceptible population, we optimise the objective functional by setting the other control to zero. This has a very small effects on susceptible and treated populations. But has an exponential effect on infected and treatment population as shown in Figure 5 and 6 respectively.

There have been an decrease in exposed population as a result of education oe sensitisation and a decrease in the number of population infected with the disease as indicated in Figure 6.

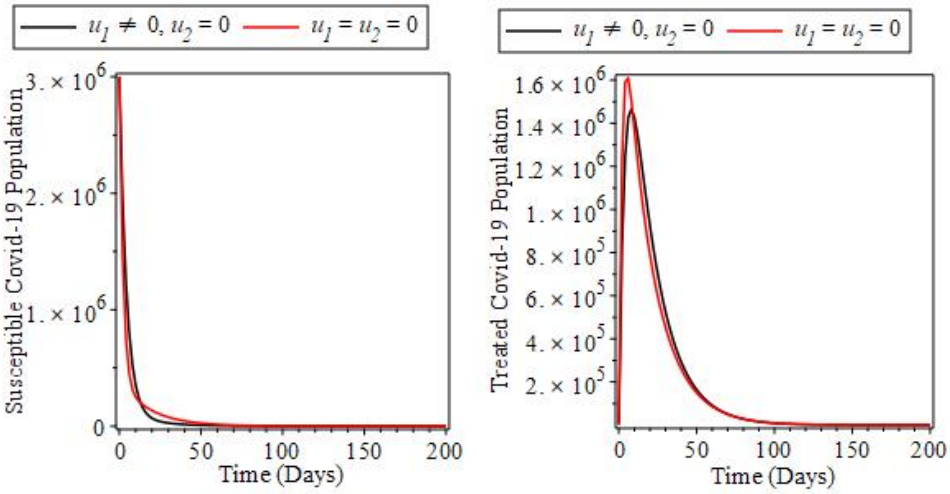

FIGURE 5. plot of phase portraits with u_1 and u_2

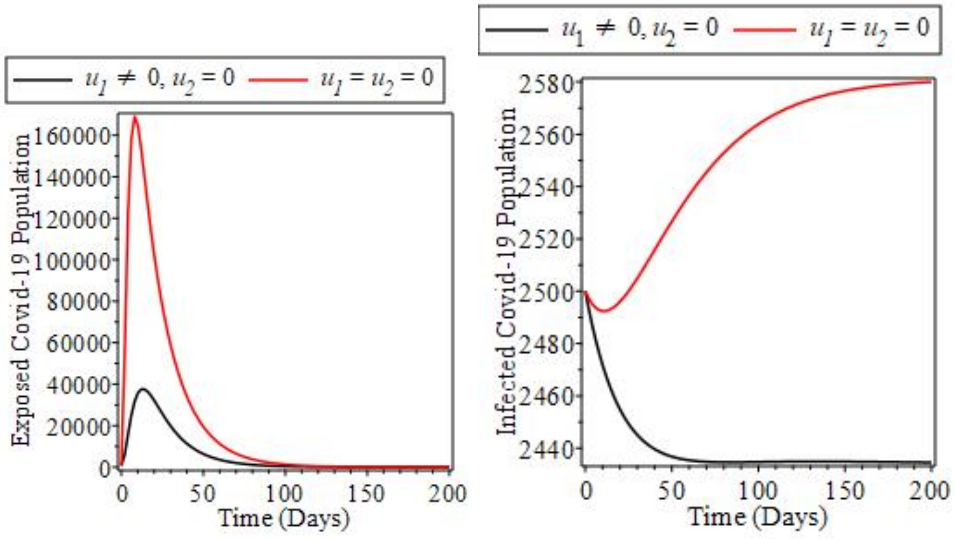

FIGURE 6. plot of phase portraits with u_1 and u_2

9. CONCLUSION

In this study, we developed a Covid-19 that explains the transmission mechanism of the disease. Model's equilibrium points were determined and local stability analyses of the model at equilibrium points was carried out. The analyses showed that disease free-equilibrium is stable when $R_0 < 1$ and unstable when $R_0 > 1$. Global stability analyses was also performed for the models using analytic methods of Lyapunov function approach.

The model is then extended to optimal control by adding time-dependent controls. Numerical simulations was carried out for the model by designing an iterative scheme that used a fourth-order Runge-Kutta method. The best strategy is education and sensitisation of the public on the dangers and possible causes of the infection.

Using vaccination as a control on susceptible population, this has an effect on susceptible, exposed, treated, and Covid-19 infected populations as shown in Figure 3 and 4 respectively. Moreover, population exposed to the infection have reduced exponentially as indicated in Figure 4.

Using education as a control on susceptible population, this has a very small effects on susceptible and treated populations. But has an exponential effect on infected and treatment population as shown in Figure 5 and 6 respectively. There have been an decrease in exposed population as a result of education and a decrease in the number of population infected with the disease as indicated in Figure 6.

ACKNOWLEDGMENT

Authors deeply appreciated the support from faculty towards the preparation of this manuscript. Much appreciation to other researchers for their numerous review comments and suggestions. Authors have expressed their profound gratitude for such a wonderful support.

SOURCE OF FUNDING

There are no sources of funding for this research. Authors are completely responsible towards the entire cost of this research.

DATA AVAILABILITY STATEMENT

The data used in the analysis of this study is taken from published articles and are cited in this paper. These published articles are also cited at relevant places within the text as references.

CONFLICT OF INTERESTS

The authors declare that there is no conflict of interests.

REFERENCES

[1] M.V. Barbarossa, J. Fuhrmann, J.H. Meinke, et al. Modeling the spread of COVID-19 in Germany: Early assessment and possible scenarios, PLoS ONE. 15 (2020), e0238559. https://doi.org/10.1371/journal.pone.0238559.

[2] V. Vytla, S.K. Ramakuri, A. Peddi, K. Kalyan Srinivas, N. Nithish Ragav, Mathematical models for predicting Covid-19 pandemic: a review, J. Phys.: Conf. Ser. 1797 (2021), 012009. https://doi.org/10.1088/1742-6596/1797/1/012009.

[3] P. Samui, J. Mondal, S. Khajanchi, A mathematical model for COVID-19 transmission dynamics with a case study of India, Chaos Solitons Fractals. 140 (2020), 110173. https://doi.org/10.1016/j.chaos.2020.110173.

[4] D. Otoo, I.O. Abeasi, S. Osman, et al. Mathematical modeling and analysis of the dynamics of hepatitis B with optimal control, Commun. Math. Biol. Neurosci. 2021 (2021), 43. https://doi.org/10.28919/cmbn/5733.

[5] W.M. Onsongo, E.D. Mwini, B.N. Nyanaro, et al. The dynamics of psittacosis in human and poultry populations: a mathematical modelling perspective, J. Math. Comput. Sci. 11 (2021), 8472-8505. https://doi.org/10.28919/jmcs/6715.

[6] H. Tessema, I. Haruna, S. Osman, et al. A mathematical model analysis of marriage divorce, Commun. Math. Biol. Neurosci. 2022 (2022), 15. https://doi.org/10.28919/cmbn/6851.

[7] S. Osman, A.Y. Omari-Sasu, R.K. Boadi, Logit model for the determinants of drug driving in Ghana, Int. J. Stat. Appl. 6 (2016), 339–346.

[8] L. Matrajt, T. Leung, Evaluating the effectiveness of social distancing interventions to delay or flatten the epidemic curve of coronavirus disease, Emerg. Infect. Dis. 26 (2020), 1740-1748. https://doi.org/10.3201/eid2608.201093.

[9] A. Zeb, E. Alzahrani, V.S. Erturk, et al. Mathematical model for coronavirus disease 2019 (COVID-19) containing isolation class, BioMed Res. Int. 2020 (2020), 3452402. https://doi.org/10.1155/2020/3452402.

[10] A. Yousefpour, H. Jahanshahi, S. Bekiros, Optimal policies for control of the novel coronavirus disease (COVID-19) outbreak, Chaos Solitons Fractals. 136 (2020), 109883. https://doi.org/10.1016/j.chaos.2020.109883.

[11] I. Ahmed, M. Ahmad, G. Jeon, Social distance monitoring framework using deep learning architecture to control infection transmission of COVID-19 pandemic, Sustain. Cities Soc. 69 (2021), 102777. https://doi.org/10.1016/j.scs.2021.102777.

[12] G.T. Tilahun, O.D. Makinde, D. Malonza, Co-dynamics of Pneumonia and Typhoid fever diseases with cost effective optimal control analysis, Appl. Math. Comput. 316 (2018), 438-459. https://doi.org/10.1016/j.amc.2017.07.063.

[13] O.D. Makinde, Adomian decomposition approach to a SIR epidemic model with constant vaccination strategy, Appl. Math. Comput. 184 (2007), 842-848. https://doi.org/10.1016/j.amc.2006.06.074.

[14] T.W. Karanja, S. Osman, M. Wainaina, Analysis and modelling of ringworm infections in an environment, Glob. J. Pure Appl. Math. 15 (2019), 649–665.

[15] S. Osman, H.A. Togbenon, D. Otoo, Modelling the dynamics of campylobacteriosis using nonstandard finite difference approach with optimal control, Comput. Math. Meth. Med. 2020 (2020), 8843299. https://doi.org/10.1155/2020/8843299.

[16] O.D. Makinde, K.O. Okosun, Impact of chemo-therapy on optimal control of malaria disease with infected immigrants, Biosystems. 104 (2011), 32-41. https://doi.org/10.1016/j.biosystems.2010.12.010.

[17] S. Osman, G. T. Tilahun, S.D. Alemu, et al. Analysis of the dynamics of rabies in North Shewa, Ethiopia, Italian J. Pure Appl. Math. 48 (2022), 877-902.

[18] S. Osman, E.A. Musyoki, R.M. Ndungu, A mathematical model for the transmission of measles with passive immunity, Int. J. Res. Math. Stat. Sci. 6 (2019), 1–8.

[19] K.O. Okosun, O.D. Makinde, A co-infection model of malaria and cholera diseases with optimal control, Math. Biosci. 258 (2014), 19-32. https://doi.org/10.1016/j.mbs.2014.09.008.

[20] D. Otoo, I.O. Abeasi, S. Osman, et al. Stability analysis and modeling the dynamics of hepatitis b with vaccination compartment, Italian J. Pure Appl. Math. 48 (2022), 903-927.

[21] S. Osman, O.D. Makinde, D.M. Theuri, Mathematical modelling of listeriosis epidemics in animal and human population with optimal control, Tamkang J. Math. 51 (2020), 261-287. https://doi.org/10.5556/j.tkjm.51.2020.2860.

[22] S. Osman, O.D. Makinde, A mathematical model for coinfection of listeriosis and anthrax diseases, Int. J. Math. Math. Sci. 2018 (2018), 1725671. https://doi.org/10.1155/2018/1725671.

[23] D. Otoo, S. Osman, S.A. Poku, et al. Dynamics of tuberculosis (TB) with drug resistance to first-line treatment and leaky vaccination: a deterministic modelling perspective, Comput. Math. Meth. Med. 2021 (2021), 5593864. https://doi.org/10.1155/2021/5593864.

[24] L.S. Pontryagin, V.G. Boltyanskii, R.V. Gamkrelidze, et al. LS pontryagin selected works: the mathematical theory of optimal processes, Routledge, 2018.

[25] W.H. Fleming, R.W. Rishel, Deterministic and stochastic optimal control, Vol. 1, Springer, New York, 2012.

[26] D. Otoo, E.K. Donkoh, J.A. Kessie, Estimating the basic reproductive number of COVID-19 cases in Ghana, Eur. J. Pure Appl. Math. 14 (2021), 135–148. https://doi.org/10.29020/nybg.ejpam.v14i1.3850.

[27] D. Dwomoh, S. Iddi, B. Adu, et al. Mathematical modeling of COVID-19 infection dynamics in Ghana: Impact evaluation of integrated government and individual level interventions, Infect. Dis. Model. 6 (2021), 381-397. https://doi.org/10.1016/j.idm.2021.01.008.